Window of visibility: a psychophysical theory of fidelity in time-sampled visual motion displays

Andrew B. Watson, Albert J. Ahumada, Jr., and Joyce E. Farrell*

Perception and Cognition Group, NASA Ames Research Center, Moffett Field, California

Received July 15, 1985; accepted November 15, 1985

Many visual displays, such as movies and television, rely on sampling in the time domain. We derive the spatiotemporal-frequency spectra for some simple moving images and illustrate how these spectra are altered by sampling in the time domain. We construct a simple model of the human perceiver that predicts the critical sample rate required to render sampled and continuous moving images indistinguishable. The rate is shown to depend on the spatial and the temporal acuity of the observer and on the velocity and spatial-frequency content of the image. Several predictions of this model are tested and confirmed. The model is offered as an explanation of many of the phenomena known as *apparent motion*. Finally, the implications of the model for computer-generated imagery are discussed.

INTRODUCTION

A film of an object in motion presents us with a sequence of static views, yet we usually see the object moving smoothly across the screen. This and other varieties of *apparent motion* have fascinated and challenged psychologists for more than a century.[1-6] It has also become a problem of considerable applied as well as theoretical interest with the advent of computer-generated displays. The applied question is: How often must we present a new view for the stroboscopic display to simulate smooth motion faithfully? The theoretical question may be stated: How can a sequence of stationary images simulate smooth motion, and why is this particular strobe rate required?

Previous attempts to answer these questions have suffered in part from lack of an objective measure of how well the stroboscopic display simulates a continuous display. The strictest possible criterion for fidelity is considered here: the ability of a human observer to discriminate visually, by whatever means, between stroboscopic and continuous displays. This permits us to determine the conditions under which stroboscopic and continuous motion are visually identical. The perceptual identity of continuous and stroboscopic displays is then explained in terms of the known spatial and temporal properties of the human visual system.

This explanation could take either of two forms. We could examine the stimuli and visual mechanisms in terms of their representation in space and time or in terms of spatial and temporal frequency. Although the two explanations are equivalent, the explanation is simpler in the frequency domain. Fahle and Poggio[7] have applied a similar frequency analysis to moving hyperacuity targets.

TIME-SAMPLED MOVING IMAGES

In a stroboscopic display the stimulus is a time-sampled version of a corresponding real motion. For example, to create the appearance of a vertical line with unit contrast moving smoothly to the right at a velocity r, we present a succession of brief views of the line, each following the other by an interval of time Δt, each displayed to the right by a distance $\Delta x = r\Delta t$. The sampling frequency w_s is the inverse of the time between presentations ($w_s = 1/\Delta t$). In addition, each sample is presented with contrast Δt, so that the time-average contrasts of smooth and sampled versions are equated. Figure 1(a) plots the position of the smoothly moving line as a function of time; the graph is a line through the origin with slope r. Figure 1(b) shows the corresponding graph for the sampled version; it is a sequence of points lying along a line through the origin with slope r.

CONTRAST DISTRIBUTION OF CONTINUOUS MOTION

Figures 1(a) through 1(d) show the contrast distributions and frequency spectra for smooth and stroboscopic motion. The points and lines in the graphs should be regarded as impulses and line impulses projecting out from the page. For example, the contrast distribution for the smoothly moving line [Fig. 1(a)] is

$$l(x, t) = \delta(x - rt), \tag{1}$$

where $l(x, t)$ specifies the contrast in the line at each point in horizontal space x and time t and where δ is the impulse function. The function $l(x, t)$ is a line impulse in the x, t space.

CONTRAST DISTRIBUTION OF STROBOSCOPIC MOTION

The stroboscopic presentation is accomplished by presenting the line briefly every Δt sec at a contrast of Δt. This amounts to multiplying by a sampling function

$$s(t) = \Delta t \sum_{n=-\infty}^{\infty} \delta(t - n\Delta t). \tag{2}$$

This has the effect of exposing the line only at times that are integral multiples of Δt. Then the stroboscopic moving line is given by

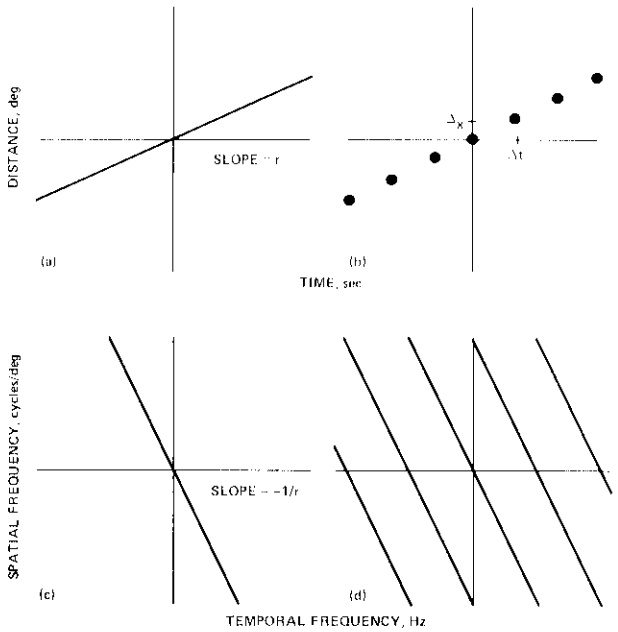

Fig. 1. Graphs and spectra of smooth and sampled lines. Points and lines should be viewed as impulses and line impulses projecting out from the page. (a) The distribution of contrast over space and time of a line moving smoothly to the right at a velocity r deg/sec. The distribution is $\delta(x - rt)$, where δ is the impulse function. (b) Contrast distribution of a sampled version of the moving line. The points indicate the times and positions at which the samples are presented. The distribution is $\Delta t\delta(x - rt)\ \Sigma_{n=-\infty}^{\infty}\ \delta(t - n\Delta t)$. (c) The spatiotemporal-frequency spectrum of the smoothly moving line. To create a smoothly moving line from sinusoidal components we require that all spatial frequencies and their temporal frequencies increase in proportion to the spatial frequency. The spectrum is $\delta(w + ur)$, where w is temporal frequency in hertz and u is spatial frequency in cycles per degree. (d) The spectrum of the time-sampled moving line is identical to the spectrum in (c), except for the addition of parallel replicas at intervals of w_s. The spectrum is $\Sigma_{n=-\infty}^{\infty}\ \delta(w + ur - nw_s)$. A similar analysis of spectra of smooth and sampled motion has been provided by Fahle and Poggio.[7]

$$l_s(x, t) = l(x, t)s(t) = \Delta t\delta(x - rt) \sum_{n=-\infty}^{\infty} \delta(t - n\Delta t). \quad (3)$$

This contrast distribution for sampled motion is shown in Fig. 1(b). It is a sequence of impulses, separated by Δx in the x dimension and Δt in the t dimension. Notice that each impulse is multiplied by Δt, so that the contrast per unit time and space is the same in smooth and sampled images.

FREQUENCY SPECTRUM OF CONTINUOUS MOTION

These distributions may be Fourier transformed to provide a description of the spatial- and temporal-frequency components that make up each stimulus. The transform of the smoothly moving line $L(u, w)$ is easily determined by application of the shift theorem

$$\begin{aligned} L(u, w) &= FT_{x,t}[l(x, t)] \\ &= FT_{x,t}[\delta(x - rt)] \\ &= FT_t \exp(-i2\pi rtu) \\ &= \delta(w + ru), \end{aligned} \quad (4)$$

where FT indicates the Fourier transform, u is the horizontal spatial frequency in cycles per degree, and w is the temporal frequency in hertz. Figure 1(c) shows that this spectrum is a line impulse passing through the origin with a slope of $-r^{-1}$.

An intuitive derivation of this result is revealed in the construction of a *stationary* line from sinusoidal components. Figure 2 illustrates how this is done by adding together an infinity of sinusoids, all with peaks coinciding at the position of the desired line. At that position, the many sinusoids add up to form the impulse; at all other points their values sum to zero. To make this line move, each sinusoid must be translated at the same velocity, so that the peaks continue to coincide at the location of the line. But the temporal frequency of a sinusoid in motion is equal to the product of its spatial frequency and its velocity ($w = ur$), so the temporal frequency of each sinusoid making up the line must increase in proportion to spatial frequency, with a proportionality constant of r [see Fig. 1(c)].

FREQUENCY SPECTRUM OF STROBOSCOPIC MOTION

To find the transform of the sampled motion, we use the convolution theorem

$$\begin{aligned} L_s(u, w) &= FT_{x,t}[l_s(x, t)] \\ &= FT_{x,t}[s(t)l(x, t)] \\ &= S(w) * L(u, w) \\ &= \delta(w + ru) * \sum_{n=-\infty}^{\infty} \delta(w - n/\Delta t) \\ &= \sum_{n=-\infty}^{\infty} \delta(w + ru - nw_s). \end{aligned} \quad (5)$$

This transformation is shown in Fig. 1(d). It is the same as that for smooth motion, except for the addition of parallel replicas at intervals of w_s Hz.

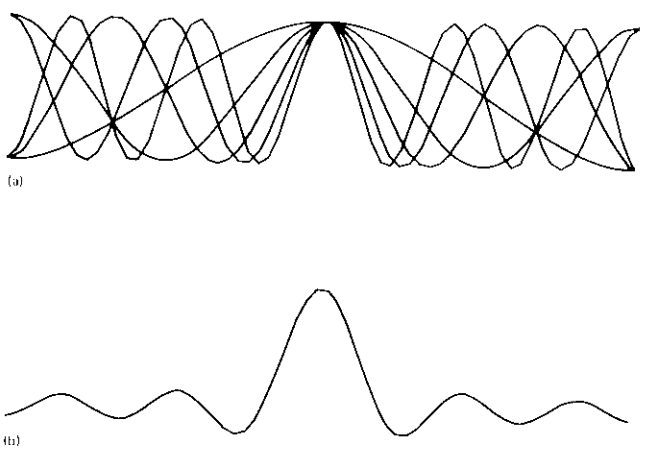

Fig. 2. Line constructed from sinusoids. (a) Five sinusoids whose peaks superimpose at a point. (b) The result of adding the five sinusoids together and dividing by five.

WINDOW OF VISIBILITY

It has been known since Shade's[8] work in 1958 that the human eye is not equally sensitive to contrast variation at all spatial frequencies and that sinusoidal variations above a critical spatial frequency are invisible. Similarly, de Lange[9] showed that temporal contrast fluctuations more rapid than a critical temporal frequency are not seen. These limits to spatial- and temporal-frequency sensitivity will be called u_l and w_l, respectively. These two limits have been shown to be relatively independent of each other: The spatial limit does not depend much on the temporal frequency of the stimulus and vice versa.[10,11] This permits us to approximate the limits of human visual sensitivity to spatial and temporal frequencies by a *window of visibility* (Fig. 3). (This rectangular window should be compared to the approximately rectangular outer *isosensitivity* contours in Fig. 3 of Koenderink and van Doorn.[11]) Components that lie within the window may be more or less visible, but those that lie outside are invisible. This description of spatiotemporal contrast sensitivity is a simplification, but it allows the generation of simple predictions that capture the essential features of the data and that are more than adequate in applied situations. These predictions follow from a reasonable conjecture. We hypothesize that two *stimuli* will appear *identical* if their *spectra*, after passing through the window of visibility, are *identical*.

A more precise expression of this hypothesis is that the spatiotemporal distribution of contrast in the image is filtered at some stage in the visual system. The limits of the passband of this filter are u_l and w_l. If, after passing through the filter, the two stimuli are identical, then an observer relying on the output of this filter will be incapable of distinguishing between the two.

CRITICAL SAMPLING FREQUENCY

Note that the spectrum of the sampled line differs from that of the smooth line only by the addition of the parallel replicas at intervals of the sampling frequency. The conjecture above implies that if these replicas lie outside the window of visibility, then the smoothly moving line and the sampled line will be indistinguishable. The replicas may be moved outside the window of visibility either by increasing the sampling frequency (which moves the replicas farther from the origin) or by reducing the velocity (which makes the replicas more early vertical). More precisely, note that for any velocity, the critical sampling frequency will be achieved when the first spectral replica is just touching the corner of the window of visibility, as is shown in Fig. 4. The coordinates of this corner are (u_l, w_l); the slope of the line impulse is $-r^{-1}$, and it intersects the w axis at the point $(w_s, 0)$. From this information it is simple algebra to relate the sampling frequency to r, u_l, and w_l. Specifically, the critical sampling frequency, w_c, at which smooth and sampled motions become indistinguishable is given by

$$w_c = w_l + ru_l. \tag{6}$$

Thus the predicted critical sampling frequency is a linear function of velocity, with an intercept given by the temporal-frequency limit and a slope given by the spatial-frequency limit.

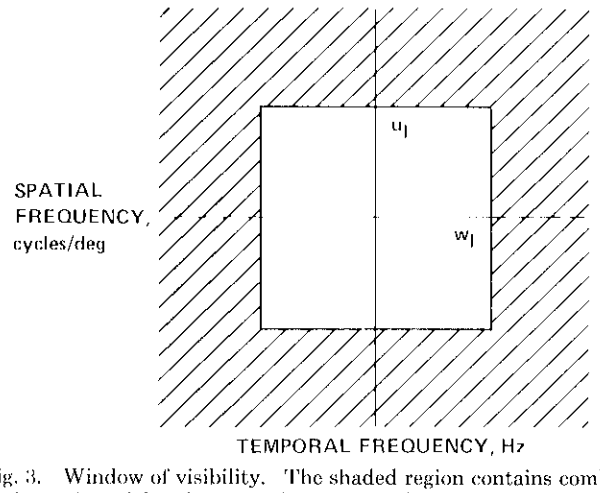

Fig. 3. Window of visibility. The shaded region contains combinations of spatial and temporal frequency that are invisible to the human eye. The window is bounded by u_l and w_l, the limits of spatial and temporal resolution.

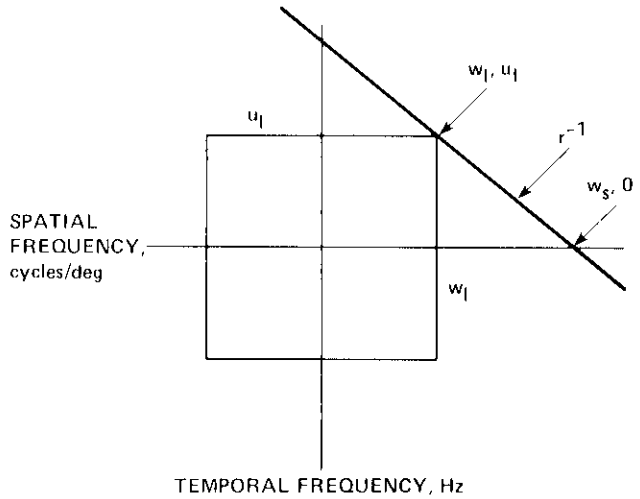

Fig. 4. Boundary condition for identical appearance of smooth and stroboscopic motion. For clarity, only the first spectral replica on the right is shown. It is just touching the corner of the window of visiblity.

EXPERIMENT 1

This prediction was tested by means of a two-interval forced-choice experiment. One interval contained a line that moved smoothly to the right or the left; the other interval contained a line moving at the same velocity but sampled at a rate of w_s. The observer was asked to choose which interval contained the sampled version and was informed after each trial whether the choice was correct. The smooth line was in fact sampled at 1920 Hz. This is effectively smooth, given the spatial and temporal transfer properties of the cathode-ray display. The stimulus was a vertical line 50 min of arc in length and 0.65 min wide that moved horizontally at the specified velocity. Observers fixated a point at the center of the path of travel. The distance traveled was $\sqrt{r}\,5/4$ deg, and the duration $5/(4\sqrt{r})$ sec. Viewing was binocular with natural pupils from a distance of 2 m. Both observers were corrected myopes. Background luminance was 50 cd m^{-2}. Stimuli were generated on an Evans and

Sutherland PS I caligraphic display. The spatial contrast of each sample in the smooth line was 200% and in the sampled line ($1920/w_s$) 200%, so that the two versions were equated for time-average contrast. The order of presentation was randomized on each trial, and the direction of motion was randomized on each presentation. A session consisted of 25 trials at each of five sampling frequencies, all at a single velocity. From the frequency of correct responses as a function of sampling frequency, the critical sampling frequency was estimated at which the observer was correct 75% of the time.

Figure 5 shows the estimates of critical sampling frequency as a function of velocity for two observers. In each case the critical sampling frequency increases approximately linearly with velocity, as predicted by Eq. (6). For both observers the intercept is at about 30 Hz, which is a good estimate for the temporal-frequency limit (w_l) under these conditions. The slope of the curve, which according to theory is an estimate of the spatial-frequency limit (u_l), is 6 cycles/deg for one observer and 13 cycles/deg for the other. These are somewhat low for estimates of the spatial-frequency limit but are not unreasonable given the low contrast and brief duration of the frequency component presumably serving to distinguish between smooth and sampled versions. Thus the data in Fig. 5 support the hypothesis that smooth and sampled motion are visually indistinguishable when the spectral components that differ between them lie outside the window of visibility.

To make a more precise prediction, it is necessary to know the bandwidth of the detector (or detectors) that discriminate between the smooth and the sampled motions. Without this information, the required contrast of the line cannot

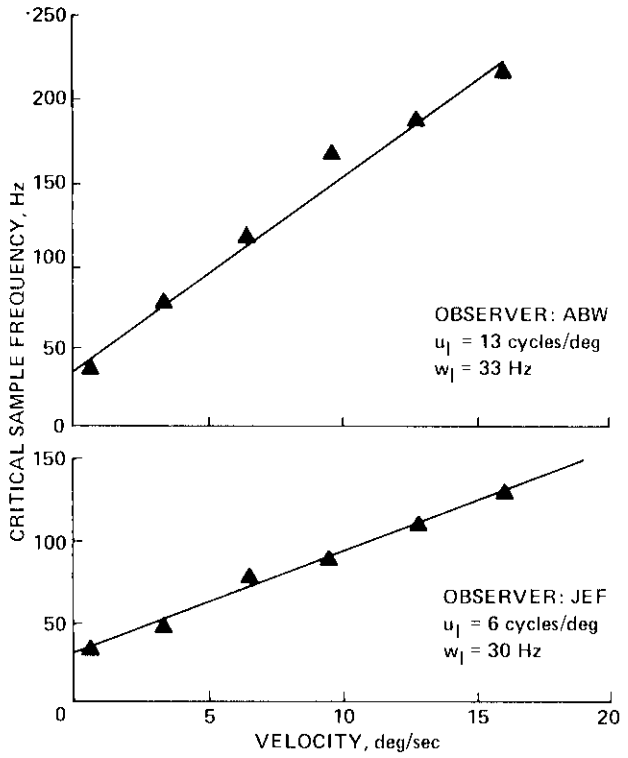

Fig. 5. Critical sampling frequency for stroboscopic motion as a function of velocity for two observers. The straight lines are fitted by eye. The slope (u_l) and the intercept (w_l) of each line are indicated.

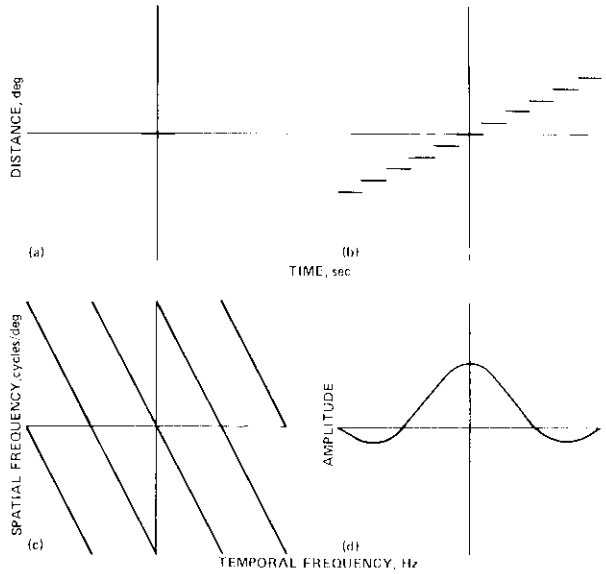

Fig. 6. Derivation of the frequency spectrum of staircase motion. (a) The stair function is a unit pulse in t multiplied by an impulse in x. (b) The contrast distribution of staircase motion is the convolution of the stair function with the stroboscopic-motion function pictured in Fig. 1(b). (c) Frequency spectrum of the stroboscopic-motion function. (d) Frequency spectrum of the stair function, a sinc function with its first zero at w_s.

be derived from the contrast sensitivity to a sinusoidal grating. For example, a detector of 1-octave bandwidth[12,13] centered at 10 cycles/deg will respond equally to the first spectral replica of the line at 200% contrast and to a sinusoidal grating with 37% contrast. Quantitative predictions would also have to take into account the detailed shape of the window of visibility, the duration of the stimulus, the inhomogeneity of spatial sensitivity across the retina, and possible masking by the spectral components lying within the window of visibility. Such predictions can be made but are beyond the scope of this report. It is partly to enable us to compute these more elaborate predictions that we have begun to construct detailed spatiotemporal models of human visual sensitivity.[13-17]

CONTRAST DISTRIBUTION OF STAIRCASE MOTION

Another effective stimulus for apparent motion is called a *staircase* presentation because of the appearance of its graph of position with respect to time. It differs from stroboscopic motion in that each presentation lasts the full interval between steps. Since this method of presentation is often used and discussed in the literature on apparent motion, it was of interest to discover whether the window-of-visibility theory could be applied to it as well.

The contrast distribution of staircase motion is derived by first constructing a function representing one stair of the staircase:

$$z(x, t) = w_s u(t w_s)\delta(x), \tag{7}$$

where $u(t)$ is the unit pulse function. The stair function is pictured in Fig. 6(a). The full staircase is constructed by convolving the stair function with the strobe function constructed earlier:

$$l_z(x, t) = l_s(x, t) * z(x, t). \quad (8)$$

This function is pictured in Fig. 6(b).

FREQUENCY SPECTRUM OF STAIRCASE MOTION

To get the transform, we again apply the convolution theorem

$$L_z(x, t) = l_s(x, t) * z(x, t). \quad (9)$$

$L_s(u, w)$ in Eq. (5) and Fig. 1(d) have already been determined and reproduced in Fig. 6(c). The transform of the stair is

$$Z(u, w) = FT_{x,t}[w_s u(w_s T)\delta(x)] = \mathrm{sinc}(w/w_s). \quad (10)$$

This function is pictured in Fig. 6(d). The transform is the product of $Z(u, w)$ and $L_s(u, w)$ that is illustrated in Fig. 7. It differs from that for stroboscopic motion in that each line impulse is "shaved off" by the same function, falling to its first zero at w_s.

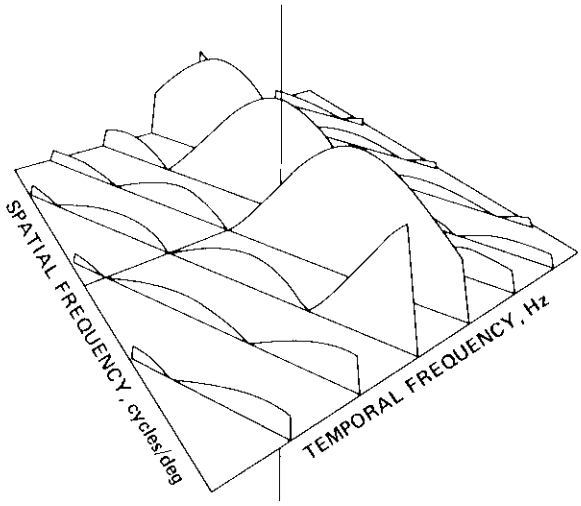

Fig. 7. Frequency spectrum of staircase motion, $L_z(u, w)$. The modulus of the spectrum is shown for clarity.

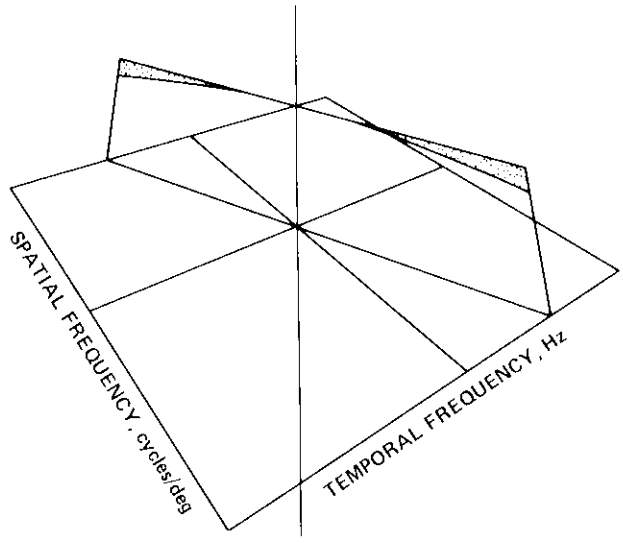

Fig. 8. Windowed spectra for stroboscopic and staircase motion when the sampling frequency is given by $w_c = w_L + ru_L$. The stippled region indicates the difference between the two. The support plane is commensurate with the window of visibility.

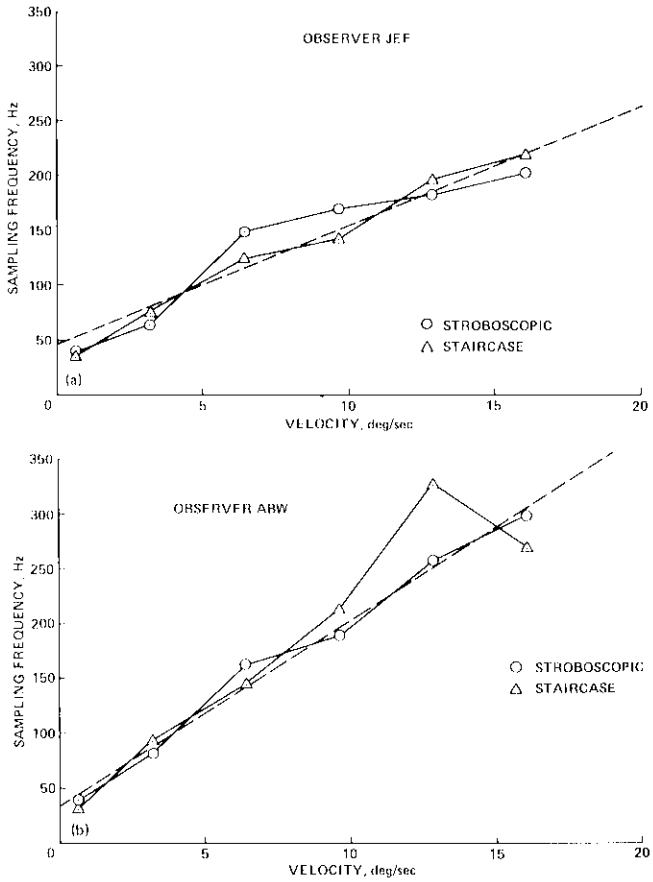

Fig. 9. Critical sampling frequency as a function of velocity for staircase and stroboscopic motion. The dashed line is a least-squares fit to the stroboscopic data (Observer ABW: intercept, 33.2 Hz; slope, 17.0 cycles/deg. Observer JEF: intercept, 46.2 Hz; slope, 11.0 cycles/deg.).

When will the staircase motion be just indistinguishable from smooth motion? As in the case of stroboscopic motion, the replicas must be kept outside the window of visibility. This leads to the same sampling requirement specified for stroboscopic motion by Eq. (6). But when this condition is met, smooth and sampled spectra still differ by the portion of the center line shaved off by the sinc function (Fig. 8). This difference (indicated by stippling in Fig. 8) is never more than 12% of the total spectrum and is usually much less. Furthermore, this difference lies in a region in which sensitivity within the window is low. It therefore seems unlikely that critical sampling frequency for staircase motion should differ much from that for stroboscopic motion.

EXPERIMENT 2

To test this prediction, experiment 1 was repeated for stroboscopic and staircase motion. For staircase motion the line was presented for the full interval between samples (Δt). The stroboscopic case was repeated because thresholds were collected by a method of adjustment rather than by the forced-choice method used in experiment 1. In the adjustment method, the observer was presented with a sequence of alternating smooth and sampled motions and was asked to

adjust the sampling frequency until the two appeared just discriminable.

The results for two observers are shown in Fig. 9. The important observation is as predicted, that staircase and stroboscopic presentation require the same critical sampling rate. The stroboscopic data collected with method of adjustment are very similar to the forced-choice data of experiment 1.

SPATIAL DEPENDENCE OF THE CRITICAL SAMPLING FREQUENCY

The spatial stimulus thus far considered is a narrow line that has spatial frequencies extending well beyond the window of visibility. When the stimulus contains a restricted range of spatial frequencies, the predictions change somewhat. Consider the case of a stimulus band limited to below u_0 cycles/deg. The spectrum will again lie along a line with a slope of $-r^{-1}$, but it will terminate at u_0 and $-u_0$. When this stimulus is presented stroboscopically at the critical sampling frequency, the situation diagrammed in Fig. 10 will result. The first replica just touches the window when

$$w_c = w_l + ru_0. \tag{11}$$

Note that this situation is the same as that for Eq. (6), except that the spatial border of the window u_l has been replaced by the spatial border of the stimulus u_0. It therefore seems appropriate to generalize and say that the spatial-frequency term in Eq. (11) should be regarded as the highest effective spatial frequency in the stimulus. This quantity will be given by the limit of the window or the stimulus, whichever is lower.

EXPERIMENT 3

This prediction was tested by asking observers to distinguish between two vertical sinusoidal gratings that drifted at the same rate (one effectively smooth and the other sampled at some rate). The use of gratings permits particularly simple predictions, since the critical sampling frequency should be equal to the temporal-frequency limit plus the velocity times the spatial frequency of the grating.

The gratings were presented at a 20% contrast on a 50-cd m^{-2} background (P31 phosphor). Display frame rate was

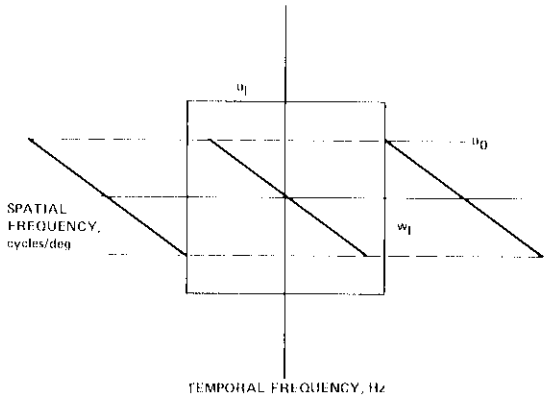

Fig. 10. Boundary conditions for a moving stimulus spatially band limited to below u_0 cycles/deg. The slope of the spectrum is $-r^{-1}$. The first replica is just touching the window of visibility at the point $w_l u_0$.

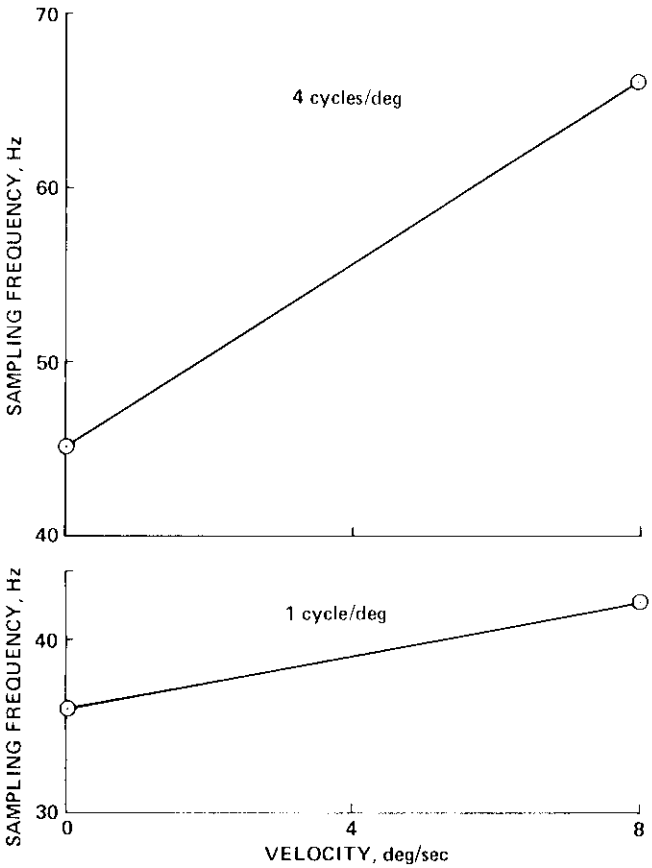

Fig. 11. Critical sampling frequency for stroboscopically moving gratings. Data are for observer DW.

200 Hz, so sampling frequencies were limited to integral divisors of this rate (100, 66.7, 50, 40, 33.3, 28.6, and 25 Hz), thus limiting the range of velocities that could be examined and the accuracy with which critical frequency could be estimated. Otherwise, conditions were similar to those in experiment 1. These results are shown in Fig. 11.

Figure 11 (bottom) shows data for a grating of 1 cycle/deg. Between 0 and 8 deg/sec the sample frequency rises by about 6 Hz, close to the predicted value of 8 Hz. Figure 11 (top) shows data for 4 cycles/deg. Between 0 and 8 cycles/deg, the sample frequency rises by about 25 Hz, close to the predicted value of 32 Hz.

RELATION TO APPARENT MOTION

It has been shown that stroboscopic and staircase motion, in which a long sequence of many views is presented to the observer, are explained by the spatiotemporal-filtering action of the eye. These two cases constitute the most compelling varieties of apparent motion. However, many classic instances of apparent motion use only two samples or two samples in repeated alternation. In such displays, the illusion has been reported to occur over distances of several degrees and time intervals of several hundred milliseconds,[3] well outside the limits for perfect fidelity discovered here. But two-sample displays evidently produce an illusion much inferior to that obtained with many samples.[18] It remains to be seen whether such displays are indistinguishable from a

corresponding real motion and whether their appearance can be explained by the theory presented here. It may be possible, however, that after passage through the visual passband filter discussed above, such stimuli are no longer discontinuous in space or time.

Morgan[4-6] has also proposed a filter theory of apparent motion, but it takes as input the function relating displacement to time rather than the function relating contrast to space and time. His filter is therefore purely temporal and does not predict the relation among critical sampling rate, velocity, and spatial frequency discovered here.

RELATION TO MODELS OF MOTION

It should be emphasized that the theory outline above is not a theory of motion sensing, since the filter represented by the window of visibility determines only what signals are admitted to the brain, not how those signals are subsequently analyzed. That is more a question of what processing and partition of signals occurs *within* the window. In particular, a motion-sensing system should be selective for direction and, perhaps, for speed. Fahle and Poggio[7] and Watson and Ahumada[19,20] have outlined some aspects of how these selectivities might be arranged in the frequency domain, and subsequent work has lead to a number of explicit models of human visual motion sensing.[16,21,22] The notion from this paper that does extend to these models is that of examining what portions of the spectrum of a motion stimulus (real or apparent) lie within the passband of the hypothetical sensor.

IMAGE RECORDING

Many images that appear on stroboscopic displays were recorded by a camera. The camera-recording process acts as a temporal filter and thus reduces the sampling rate required in subsequent display. The filtering action occurs either because the aperture is left open for a while during each frame or because the reacting medium (film or video tube) has a finite reaction time.

To see the effect of this filtering, assume that the recording process removes all temporal frequencies above w_f. When an image moves with velocity r, its spectrum tilts in the u, w plane with slope $-r^{-1}$. Thus, as shown in Fig. 12, all spatial frequencies above $u = w_f/r$ are removed. Substituting this as the highest effective spatial frequency in Eq. (11) gives

$$w_c = w_l + r(w_f/r) = w_l + w_f. \tag{12}$$

This condition will hold whenever w_f/r is less than u_0 or u_l. Thus the sampling requirements remain constant, regardless of velocity. In effect, the amount of spatial filtering just compensates for the increased sampling rate that an increase in velocity would otherwise require. Furthermore, the spatial filtering occurs only when the image moves, so that stationary images can be viewed with high detail.

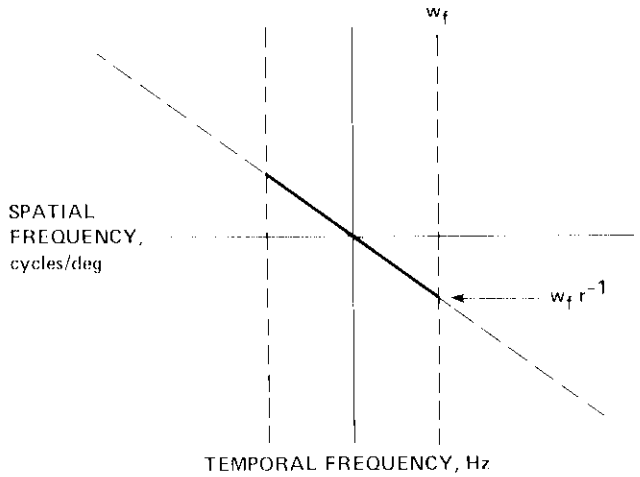

Fig. 12. The effect of temporal filtering on the spectrum of a moving image. The band limit of the temporal filter is w_f. The temporal filter removes all spatial frequencies above w_f/r.

All the cases considered above can now be summarized in one equation in which the highest effective spatial frequency is given by the least of three possible limits:

$$w_c = w_l + r \min(u_0, u_l, w_f/r). \tag{13}$$

COMPUTER-GENERATED IMAGERY

Computer-generated images bypass the camera-recording process and are not subject to the spatial and temporal prefiltering described above. In object space, that is, the coordinate space in which the image is defined internal to the computer, the image may have infinitely high spatial and temporal frequencies. It is for this reason that presentation of computer imagery on conventional television displays, with their temporal sampling frequency of 30 or 60 Hz, often gives rise to serious artifacts.

One possible solution to this problem is to simulate the recording process in the computer. This might be possible by sampling the scene at extra-high resolution, averaging the last n frames, and then sampling at the resolution of the display. However, this would require that all computations necessary to get from object space to image space (projection, hidden-line removal, surface generation, shading, etc.) be done at the extra-high resolution. An alternative strategy would be to code the image in spatial-frequency bands and then select for display only those bands that velocity and sampling frequency will not alias. This subject has lately received intense interest in the computer-graphics community, and a number of novel methods of temporal antialiasing have been proposed.[23-26] Whatever the algorithm employed, all these methods enhance the similarity between the portions of the image spectrum within the window of visibility of continuous and sampled versions.

CONCLUSIONS

The general notions presented here regarding sampled displays and visual filtering can be extended to an arbitrary spatial image undergoing an arbitrary transformation over time, and the sampling process can be extended to the two spatial dimensions as well as time. They provide answers to some long-standing puzzles in perceptual psychology and to some modern problems in advanced visual displays.

ACKNOWLEDGMENT

An earlier version of this paper was published as a NASA Technical Paper.[27]

* Present address, Hewlett-Packard, Palo Alto, California 94305.

REFERENCES

1. S. Exner, "Ueber das Sehen von Bewegungen und die Theorie des zusammengesetzen Auges," Sitzungber. Akad. Wiss. Wien **72,** 156–160 (1875).
2. O. Braddick, "A short-range process in apparent motion," Vision Res. **14,** 519–527 (1974).
3. P. A. Kolers, *Aspects of Apparent Motion* (Pergamon, New York, 1972).
4. M. J. Morgan, "Perception of continuity in stroboscopic motion: a temporal frequency analysis," Vision Res. **19,** 491–500 (1979).
5. M. J. Morgan, "Analogue models of motion perception," Phil. Trans. R. Soc. London Ser. B **290,** 117–135 (1980).
6. M. J. Morgan, "Spatiotemporal filtering and the interpolation effect in apparent motion," Perception **9,** 161–174 (1980).
7. M. Fahle and T. Poggio, "Visual hyperacuity: spatiotemporal interpolation in human vision," Proc. R. Soc. London Ser. B **213,** 451–477 (1981).
8. O. H. Shade, "Optical and photoelectric analog of the eye," J. Opt. Soc. Am. **46,** 721–739 (1956).
9. H. de Lange, "Relationship between critical flicker frequency and a set of low frequency characteristics of the eye," J. Opt. Soc. Am. **44,** 380–389 (1954).
10. J. G. Robson, "Spatial and temporal contrast sensitivity functions of the visual system," J. Opt. Soc. Am. **56,** 1141–1142 (1966).
11. J. J. Koenderink and A. J. van Doorn, "Spatiotemporal contrast detection threshold surface is bimodal," Opt. Lett. **4,** 32–34 (1979).
12. A. B. Watson, "Summation of grating patches indicates many types of detector at one retinal location," Vision Res. **22,** 17–25 (1982).
13. A. B. Watson, "Detection and recognition of simple spatial forms," in *Physical and Biological Processing of Images*, A. C. Slade, ed. (Springer-Verlag, Berlin, 1983).
14. A. J. Ahumada, Jr., and A. B. Watson, "Equivalent noise model for contrast detection and discrimination," J. Opt. Soc. Am. A **2,** 1133–1139 (1985).
15. K. R. K. Nielsen, A. B. Watson, and A. J. Ahumada, Jr., "Application of a computable model of human spatial vision to phase discrimination," J. Opt. Soc. Am. A **2,** 1600–1606 (1985).
16. A. B. Watson and A. J. Ahumada, Jr., "Model of human visual-motion sensing," J. Opt. Soc. Am. A **2,** 322–342 (1985).
17. A. B. Watson, "Temporal sensitivity," in *Handbook of Perception and Human Performance*, J. Thomas, ed. (Wiley, New York, to be published).
18. G. Sperling, "Movement perception in computer-driven visual displays," Behavior Res. Methods Instrum. **8,** 144–151 (1976).
19. A. B. Watson and A. J. Ahumada Jr., "A theory of apparently real motion," Invest. Ophthalmol. Visual Sci. Suppl. **22,** 143 (1982).
20. A. B. Watson and A. J. Ahumada, Jr., "A look at motion in the frequency domain," NASA Tech. Memo. 84352 (NASA, Washington, D.C., 1983).
21. J. P. H. van Santen and G. Sperling, "Elaborated Reichardt detectors," J. Opt. Soc. Am. A **2,** 300–321 (1985).
22. E. H. Adelson and J. R. Bergen, "Spatiotemporal energy models for the perception of motion," J. Opt. Soc. Am. A **2,** 284–299 (1985).
23. M. Potmesil and I. Chakravarty, "Modeling motion blur in computer generated images," Comput. Graphics **17,** 389–399 (1983).
24. J. Korein and N. Badler, "Temporal anti-aliasing in computer generated animation," Comput. Graphics **17,** 377–388 (1983).
25. R. Cook, T. Porter, and L. Carpenter, "Distributed ray tracing," Comput. Graphics **18,** 137–145 (1984).
26. M. A. Z. Dippe and E. H. Wold, "Antialiasing through stochastic sampling," Comput. Graphics **19,** 69–78 (1985).
27. A. B. Watson, A. J. Ahumada, Jr., and J. Farrell, "The window of visibility: a psychophysical theory of fidelity in time-sampled visual motion displays," NASA Tech. Paper 2211 (NASA, Washington, D.C., 1983).